

KINETIC STUDY OF THE THERMAL DECOMPOSITION OF TEA⁺/SAPO-5

D. F. Brito¹, E. F. B. Silva¹, D. P. Rodrigues², M. C. N. Machado^{2*}, M. A. Silva¹, V. Simões³, M. W. N. C. Carvalho³, L. E. B. Soledade², Iêda M. G. Santos² and A. G. Souza²

¹Departamento de Química, CCT, Universidade Estadual da Paraíba, CEP 58109-790 Campina Grande, PB, Brazil

²Departamento de Química, CCEN, Universidade Federal da Paraíba, CEP 58059-900 João Pessoa, PB, Brazil

³Departamento de Engenharia Química, CCT, Universidade Federal de Campina Grande, 58100-000 Campina, Brazil

A silico alumino phosphate with AFI structure (SAPO-5) was prepared in a two-phase medium and characterized by XRD, followed by the addition of TEA⁺. The kinetics of the TEA⁺/SAPO-5 thermal decomposition reaction was studied by isothermal and dynamic thermogravimetry. Two kinetic models, D₃ and D₄ based on diffusion processes were found as best to fit the isothermal data. On the other hand, the best fit for the dynamic data is the F₁ first order reaction model. According to the apparent activation energy values, the use of the dynamic method indicates a higher temperature dependence than the isothermal method.

Keywords: kinetics, SAPO-5, thermal analysis

Introduction

The kinetics of heterogeneous decomposition has been studied by dynamic and isothermal thermogravimetric methods [1]. For the A(s)→B(s)+C(g) type reactions the fundamental equation can be described as $d\alpha/dt=kf(\alpha)$. The selection of the best kinetic model is based on the mathematical–statistical treatment of the experimental results.

The silico alumino phosphate (SAPO's) molecular sieves came to light with the silicon incorporation into the aluminum phosphate structure (AlPO's) in 1984 [2]. Aluminum phosphates are microporous solids constituted by [AlO₄]⁻ and [PO₄]⁺ tetrahedra, in which the Al/P=1, leading to an electrically neutral structure. The isomorphous substitution of silicon for phosphorus leads to a negative charge along the structure, which is compensated by the molecules of the protonated template. The selection of the silico alumino phosphate (SAPO-5) with the AFI structure was based on its application as a catalyst in hydrocracking processes and other reactions that involve acid catalysis [3].

This work aims to determine the decomposition kinetics of TEA⁺/SAPO-5, based on thermogravimetric analyses performed by dynamic and isothermal methods.

Experimental

SAPO-5 synthesis in a two-phase medium

In the present work, the SAPO-5 synthesis was based on the following molar composition: 0.46 SiO₂, P₂O₅, Al₂O₃, (C₂H₅)₃N, 0.072CTMABr, 4.4hexanol, 40H₂O. The synthesis process started with the addition of phosphoric acid 85% (Merck), diluted in half of the total amount of water, into a beaker containing the pseudoboehmite (Condea), dispersed in the remaining amount of distilled water.

The beaker contents were kept under stirring for 2 h. Soon after, the template (triethylamine, 99% Merck) was added to the mixture, and stirred for 2 h. Afterwards, a solution containing tetraethyl orthosilicate (98% Aldrich, silicon source), *n*-hexanol (Merck) and the surfactant CTMABr (Merck) was added to the mixture, and kept under stirring for more 2 h. Later, the material was placed into Teflon crucibles and then conditioned in stainless steel autoclaves and placed in an oven for 18 h, at 170°C for crystallization. The resulting material was centrifuged, washed with distilled water and dried at 60°C. This synthesis procedure is presented in Fig. 1.

Methods

X-ray diffraction

The X-ray diffraction patterns were determined using a Siemens D-5000 diffractometer and CuK_α radiation, with a goniometer speed of 2° min⁻¹ and a 2θ range from 5 to 50°.

* Author for correspondence: ceicamachado3@yahoo.com.br

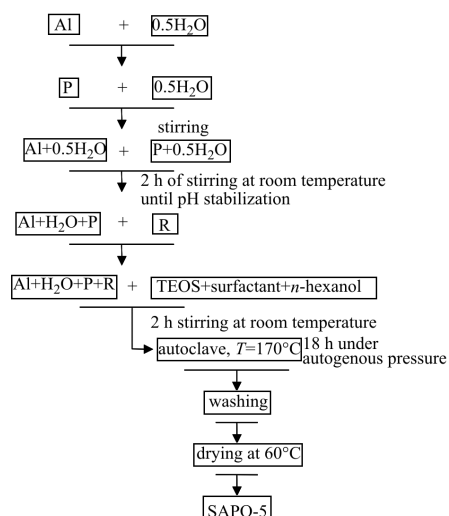


Fig. 1 Scheme of SAPO-5 synthesis in a two-phase medium

Thermal analyses

The TG curves were obtained in a TGA-50 Shimadzu thermobalance under synthetic air and employing isothermal and dynamic heating techniques. The sample mass was 10 ± 0.5 mg. The isothermal analyses were performed at 480, 500, 530 and 560°C and the dynamic curves were obtained at 5 and 10°C min⁻¹ heating rates up to 900°C.

The DSC curve was obtained in nitrogen using a DSC-50 Shimadzu Calorimeter with a heating rate of 10°C min⁻¹.

Results and discussion

Single phase API from SAPO was obtained as observed in the XRD pattern of a sample submitted to a crystallization time of 18 h (Fig. 2).

Figure 3 shows the superimposed TG, DTG and DSC curves of TEA⁺/SAPO-5 in which three mass loss steps are noticed. This behavior is typical for uncalcined zeolite compounds [4]. The data obtained from the dynamic TG curves with a heating rate

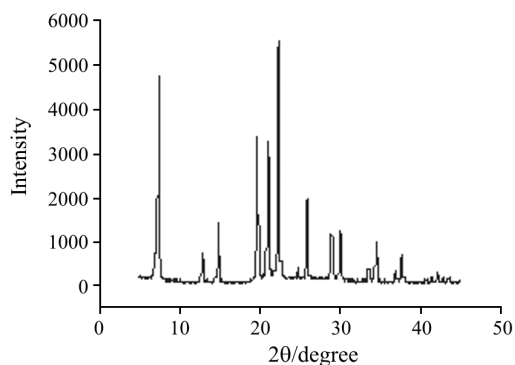
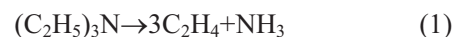


Fig. 2 XRD pattern of SAPO-5

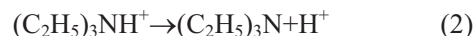
Table 1 Thermogravimetric data of TEA⁺/SAPO-5

Step	Temperature range/°C	Attributions
1 st	25–150	de-hydration
2 nd	350–490	elimination of the triethylamine
3 rd	520–750	TEA ⁺ decomposition with elimination of TEA
Residue	>750	protonated SAPO-5

of 10°C min⁻¹ are listed in Table 1. The first mass loss step, between room temperature and 150°C is related to the SAPO-5 dehydration. The second mass loss step in the 350–490°C range is ascribed to the decomposition of triethylamine (template) present within the pores and channels of the molecular sieve according to reaction (1):



The third step, between 520 and 750°C is related to the decomposition of the protonated amine (TEA⁺), according to reaction (2) with the subsequent decomposition of triethylamine as shown in reaction (1) leading to the formation of the protonated SAPO-5.



The profile of the DSC curve is characteristic of the SAPO-5 compound. The endothermic transitions are related to the desorption of water and the occluded template. It was not possible to observe the transition related to the decomposition of TEA⁺ since the DSC equipment operates only up to 550°C.

The purpose of studying the TEA⁺/SAPO-5 decomposition reaction by isothermal method is to identify the kinetic mechanism of the reaction. Another objective is to investigate the temperature dependence of the reaction by determining its apparent activation energy, *E*.

Figure 4 illustrates the variation of the decomposed fraction (α) vs. time at different temperatures. A linear relationship of α with time can be noticed at the onset of the reaction, followed by a deceleration

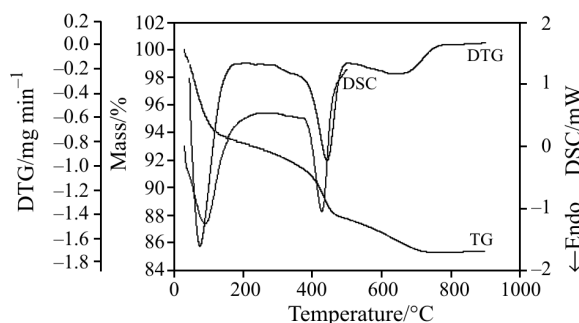


Fig. 3 Superimposed TG/DTG/DSC curves of TEA⁺/SAPO-5

Table 2 Rate constant (k) according to the equation $g(\alpha)=kt+k_0$

Model	Parameter	Isothermal temperature/°C			
		480	500	530	560
D ₃	k/s^{-1}	$1.58 \cdot 10^{-5}$	$1.60 \cdot 10^{-5}$	$3.58 \cdot 10^{-5}$	$4.79 \cdot 10^{-5}$
	r	0.99768	0.9986	0.9997	0.9966
	s	$5.50 \cdot 10^{-3}$	$4.33 \cdot 10^{-3}$	$2.1 \cdot 10^{-3}$	$6.87 \cdot 10^{-3}$
D ₄	k/s^{-1}	$1.01 \cdot 10^{-5}$	$1.03 \cdot 10^{-5}$	$2.29 \cdot 10^{-5}$	$3.10 \cdot 10^{-5}$
	r	0.99783	0.9989	0.9973	0.9996
	s	$3.41 \cdot 10^{-3}$	$2.54 \cdot 10^{-3}$	$3.8 \cdot 10^{-3}$	$1.54 \cdot 10^{-3}$

r – linear correlation coefficient, s – standard deviation of the $g(\alpha)$ function

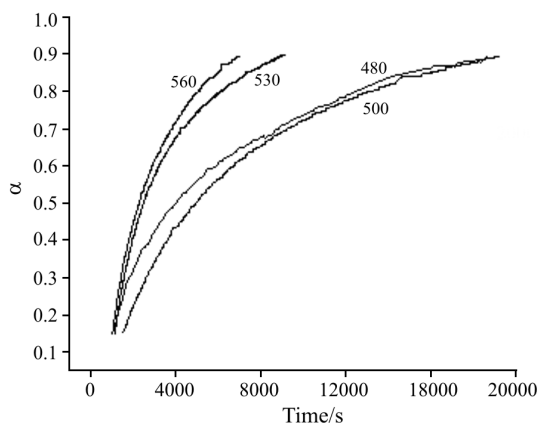
stage. This behavior can be interpreted as inherent to a process in which nucleation and growth are very fast and the reaction kinetics is governed by the elimination of the formed products through the pores and channels of the SAPO-5.

The isothermal curves were evaluated using different kinetic models of heterogeneous decomposition reactions [5–13], each one characterized by its own $g(\alpha)$ function, in order to determine the thermal decomposition mechanism of TEA⁺/SAPO-5. The experimental data were treated by linear regression techniques according to the relationship $g(\alpha)=kt+k_0$. The apparent activation energy was determined by the Arrhenius equation. The kinetic evaluation of the dynamic curves was carried out using the Coats–Redfern equation [14].

Results indicate that the best kinetic models are based on diffusion-controlled processes in agreement with the shape of the kinetic curves (Fig. 4). The best fits of the experimental data were obtained with D₃ – Jander equation (Fig. 5) and D₄ – Ginstling–Brounshtein equation (Fig. 6) models, whose $g(\alpha)$ functions are expressed by Eqs (3) and (4), respectively.

$$g(\alpha)=[1-(1-\alpha)^{1/3}]^2 \quad (3)$$

$$g(\alpha)=(1-2\alpha/3)-(1-\alpha)^{2/3} \quad (4)$$

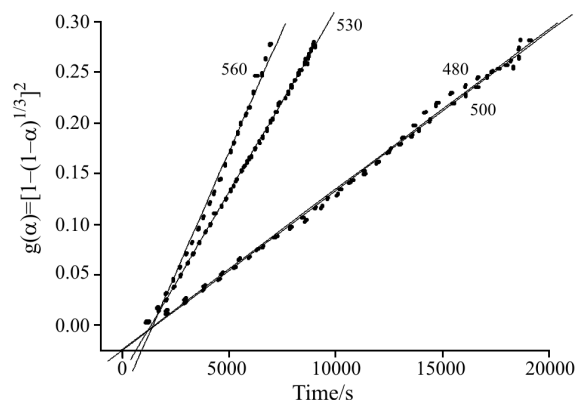
**Fig. 4** Isothermal decomposition curves of TEA⁺/SAPO-5 at different temperatures (°C)

The rate constants, the linear correlation coefficients and the standard deviations obtained from the correlations between the experimental data and theoretical values from these models are displayed in Table 2.

The models that best fitted the experimental data are physically similar, being both related to a three-dimensional diffusion controlled process. The statistical treatment showed a small difference between the standard deviation values. Therefore, although the D₄ model presented on average smaller standard deviations and higher linear correlation coefficients it is not possible to choose one of them as undoubtedly being the most appropriate for the experimental data. It should be pointed out that both models can describe the physical event. Consequently, the support of other techniques is necessary to clearly state which kinetic model describes better the process.

A study on the decomposition of TEA⁺/SAPO-5 was undertaken using the dynamic heating method with the purpose in order to investigate the reaction kinetics under different heating conditions. Two heating rates were used (5 and 10°C min⁻¹) in order to obtain a higher reliability of the kinetic parameters using thermogravimetry. The range of decomposed fraction (α) 0.15 < α < 0.95 was employed.

The α curve as a function of time (Fig. 7) presents an almost linear relationship indicating that the decomposition rate seems to be independent of the decomposed fraction.

**Fig. 5** Isothermal decomposition according to D₃ model

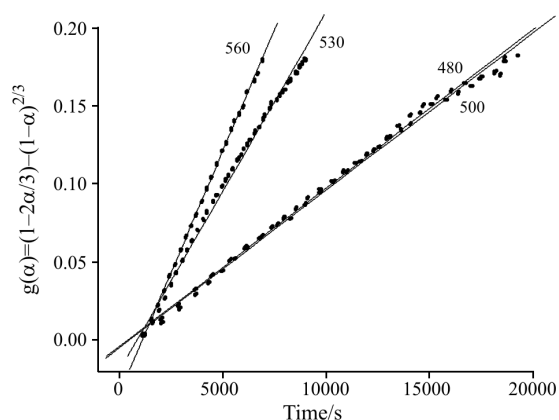


Fig. 6 Isothermal decomposition, according to the D₄ model

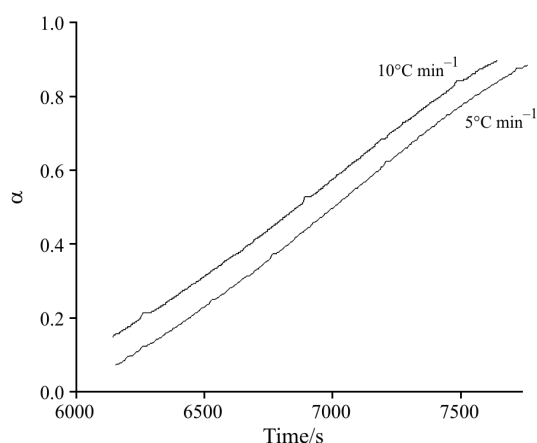


Fig. 7 Dynamic decomposition of TEA⁺/SAPO-5

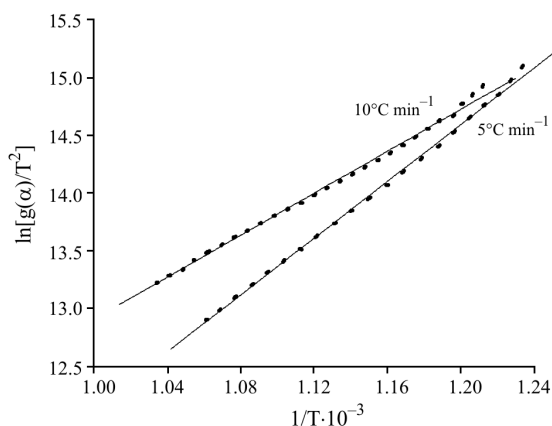


Fig. 8 Dynamic decomposition according to the F₁ model

F₁ first order reaction model was found which fitted the best of the experimental data (Fig. 8).

The apparent activation energy values estimated by the isothermal and dynamic heating methods are presented in Table 3.

The values of the apparent activation energy show that in the studied process the dynamic method indicates higher temperature dependence than the isother-

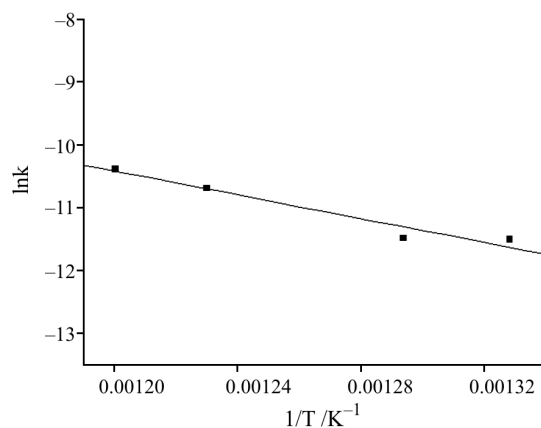


Fig. 9 Arrhenius plot of the calculated rate constants

Table 3 Kinetic parameters estimated by the isothermal and dynamic heating methods

Parameter	Method			
	isothermal		dynamic	
	D ₃	D ₄	5°C min ⁻¹	10°C min ⁻¹
<i>E</i> /kJ mol ⁻¹	81.0	78.7	102.1	100.4
<i>r</i>	0.96	0.97	0.9993	0.9988
<i>s</i>	0.19	0.16	0.024	0.030

mal method. This can be due to the inherent higher temperature gradient of the dynamic heating method.

Figure 9 shows the Arrhenius plot of the rate constant, *k*, obtained using the D₄ model. As it is shown in Table 3 the linear correlation coefficients obtained by the dynamic method are higher than the ones determined using the isothermal one.

Conclusions

The isothermal method indicated the presence of a deceleration stage – after an initial constant rate stage the reaction rate decreases as the reagent is consumed. Such deceleration was not observed in the dynamic heating method which led to an almost linear relationship between α and reaction time indicating that the reaction rate is independent of the decomposed fraction.

According to the isothermal method the kinetic models that best fitted the experimental data were the D₃ and D₄ models based on three-dimensional diffusion. On the other hand, the dynamic heating method indicated that the F₁ model based on a first order reaction is the best fitting one.

The values of the apparent activation energy show that the dynamic method indicates a higher temperature dependence than the isothermal method.

Acknowledgements

The authors acknowledge CENPES-PETROBRÁS and the Brazilian financing agencies FINEP and CNPq for the financial support of this work.

References

- 1 J. H. G. Rangel and A. G. Souza, *Thermochim. Acta*, 328 (1999) 187.
- 2 C. M. Lopes, *Segundo Curso Iberoamericano sobre Peneiras Moleculares*, CYTED, São Carlos, Brazil 1995, p. 87.
- 3 D. S. Kim, S. H. Chang and W. S. Ahn, *J. Mol. Catal. A: Chem.*, 179 (2002) 175.
- 4 M. M. Urbina, Ph.D. Thesis, Graduating Program in Chemistry, UFSCar, Brazil 1997.
- 5 H. Tanaka, S. C. Ohshima, S. Ichaiba and H. Negita, *Thermochim. Acta*, 48 (1981) 137.
- 6 J. D. Handcock and J. H. Sharp, *J. Am. Ceram. Soc.*, 55 (1972) 74.
- 7 J. H. Sharp, G. W. Brindley and A. B. N. Narahari, *J. Am. Ceram. Soc.*, 49 (1966) 379.
- 8 A. C. Norris, M. I. Poppe and M. Selwood, *Thermochim. Acta*, 41 (1980) 356.
- 9 J. M. Criado, M. Gonzalez, A. Ortega and C. Real, *J. Thermal Anal.*, 29 (1984) 243.
- 10 H. Tanaka, S. C. Ohshima and H. Negita, *Thermochim. Acta*, 53 (1982) 387.
- 11 M. M. Conceição, A. M. L. Melo, N. Narain, I. M. G. Santos and A. G. Souza, *J. Therm. Anal. Cal.*, 67 (2002) 273.
- 12 M. M. Conceição, V. J. Fernandes Jr., F. S. M. Sinfrônio, J. C. O. Santos, M. C. D. Silva, V. M. Fonseca and A. G. Souza, *J. Therm. Anal. Cal.*, 79 (2005) 461.
- 13 M. M. Conceição, A. G. Souza, M. F. S. Trindade, T. G. Nascimento, C. F. S. Aragão and R. O. Macedo, *Thermochim. Acta*, 433 (2005) 163.
- 14 A. W. Coats and J. P. Redfern, *Nature*, 201 (1964) 68.

DOI: 10.1007/s10973-006-8189-7